Wiley
Advances in Civil Engineering
Volume 2024, Article ID 5556324, 13 pages
https://doi.org/10.1155/2024/5556324

WILEY

Research Article

Evaluation of Helical Pile Performance in TRcM for Soft Ground Improvement: Insights from Field Test and Application

Kim Hyeong-Joo[1], **Ham Tae-Gew**[1], **Shamsher Sadiq**[1], **Peter Rey Dinoy**[1] and **Youn Gi-Cheol**[2]

[1]*Department of Civil Engineering, Kunsan National University, Gunsan, Republic of Korea*
[2]*TR Engineering and Construction, Uiwang 16006, Republic of Korea*

Correspondence should be addressed to Ham Tae-Gew; hamtg@kunsan.ac.kr

Received 30 August 2023; Revised 26 April 2024; Accepted 3 May 2024; Published 27 May 2024

Academic Editor: H. Naderpour

The tabular roof construction method (TRcM) is an alternative to open-cut and cover tunnels commonly used in constructing underground structures. The open-cut tunnels often lead to traffic congestion and ground settlement, especially in densely populated areas. However, when dealing with very soft ground that allows minimal settlement, piling becomes necessary to distribute the load. Implementing ground improvement solutions in such scenarios poses challenges in terms of space and time constraints. This study presents a unique case study that explores the combination of helical piles with the TRcM, offering a viable solution for ground improvement under challenging ground, limited space, and time constraint conditions. A robust helical pile loading system design for static compression tests inside TRcM ensuring TRcM pipe stability is presented. Also, the validation of the helical pile-bearing capacity interpretation using various factors through static field test inside the TRcM is presented.

1. Introduction

As urban populations grow, space becomes a scarce resource, leading to an increasing demand for developing urban underground areas. However, the value of these spaces often conflicts with the complexities of construction, particularly in densely populated regions with existing buildings and heavy traffic. Constructing shallow underground spaces can disrupt the ground environment, posing safety risks to various urban facilities. Thus, achieving safe and efficient construction while minimizing disturbances to the sensitive urban environment remains a significant challenge.

Large urban ground facilities, including ancient buildings, high-rise structures, and rail transit lines, are susceptible to deformation. Therefore, when building underground structures near such facilities, employing effective deformation control methods is crucial. For small-span structures, pipe jacking or tunnel boring machine methods are commonly used, benefitting from relatively mature settlement control technology. However, for larger structures like subway stations, the undercutting method becomes necessary, involving stress release control through various techniques. Yet, settlement compensation measures, such as grouting or mechanical lifting, pose difficulties in terms of construction complexity, effect reliability, and cost.

Addressing the aforementioned challenges, a unique underground engineering construction method utilizing large-diameter steel tube groups as load-bearing structures has been developed. This approach was first introduced in the 1970s during the construction of Antwerp Central Station in Belgium [1]. In the 1990s, Lunardi [2] proposed a similar method known as the "Cellular Arch Method," which was used in VENZIA station, Milan, Italy. South Korea further enhanced the technology, naming it the "Tubular Roof Construction Method" (TRcM), and successfully implemented it in the Lot 923 Station of Seoul Metro Line 9 in 2006 [3]. This method has also found application in China, where it is known as the new tabular roof method [4]. It was successfully implemented in projects such as the Shenyang Metro and the Taiyuan Yingze Underpass [5].

This research presents a case history of the construction of the TRcM subway site in Seoul, South Korea, where various

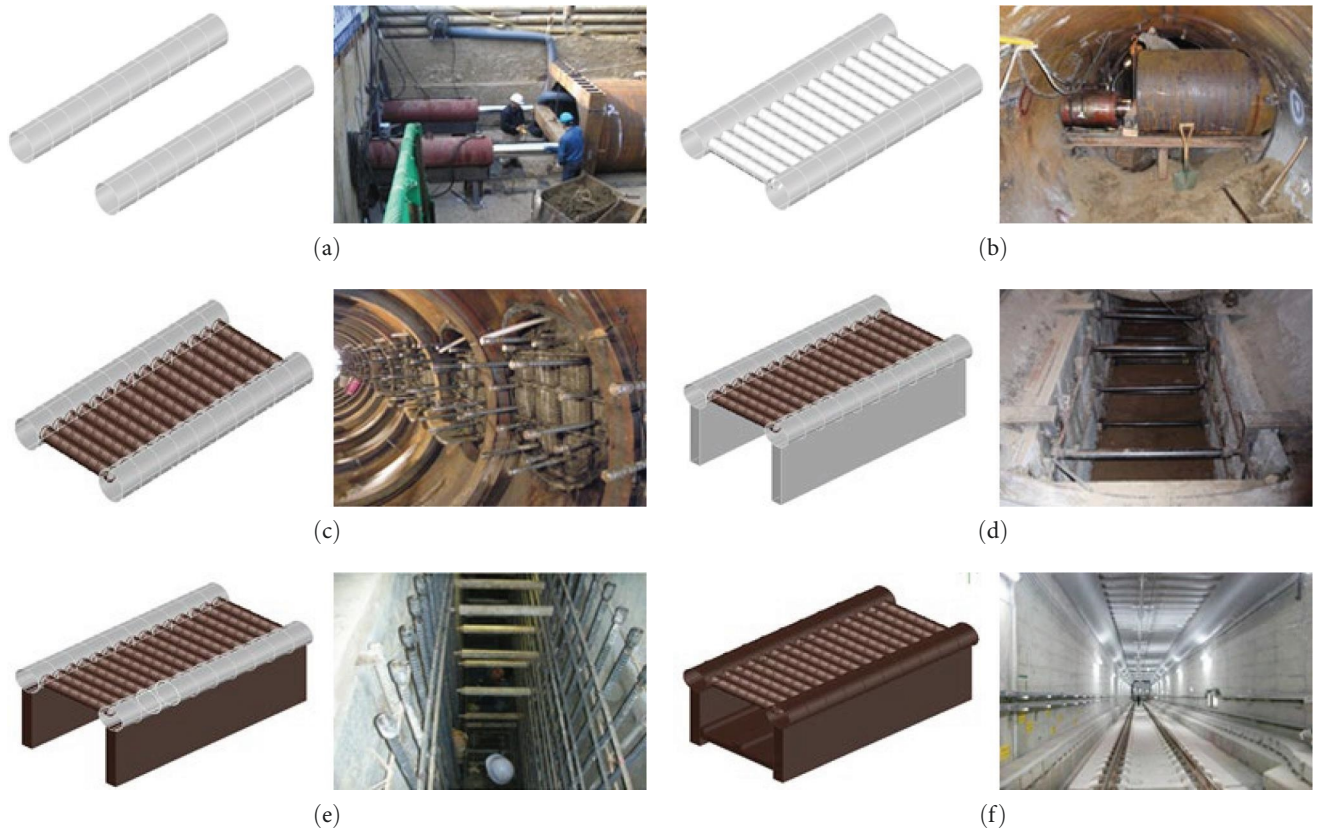

Figure 1: Illustration of TRcM construction methodology. (a) Insertion of large steel pipe, (b) insertion of transverse steel pipe gallery, (c) filling the transverse slabs, (d) trench formation by excavating soil, (e) pouring of concrete to form continous vertical walls, and (f) concreting bottom slab and the placement of railway track.

difficulties were encountered due to the soft ground geology, limited space, and time constraints. To address these challenges, a unique approach was adopted to enhance the bearing capacity of TRcM by employing helical piles. The paper introduces the use of helical piles in TRcM, the static helical pile load test inside the TRcM, as well as the evaluation of helical pile-bearing capacity factors.

2. Overview TRcM

The major differences between TRcM and traditional roof systems lie in their structural configurations. In the traditional system, small diameter pipes are utilized as forepoling for support, while the permanent lining of the main structure carries the structural load. In contrast, TRcM employs large-diameter tabular roof pipes along with permanent reinforced concrete to bear all structural loading. As a result of these distinctions, the level of roof settlement in TRcM remains well below allowable limits, unlike in traditional roof systems where these limits are often exceeded. This unique characteristic of TRcM makes it an ideal solution for closely built systems situated above or adjacent to existing subway lines, requiring minimal to no disturbance during the construction of new subway lines. However, the construction of large-diameter pipes presents a notable complexity. In environments with strict settlement criteria, there currently exists no viable alternative to this method. Another limitation of TRcM is the absence of a unified framework encompassing conceptual definitions, design principles, design specifications, and an in-depth analysis of implementations. Consequently, TRcM has yet to evolve into a fully developed technical system. This limitation also makes it challenging to find adequate references and guidelines for applying TRcM in new projects.

Constructing a tunnel using the TRcM technique offers several benefits. First, it allows normal railway traffic operations to continue during the tunnel construction. Second, it enables effective control of groundwater table drawdown during the process. The following steps explain the construction procedure of TRcM, as shown in Figure 1,

(1) The large steel gallery pipe is inserted into position using a sizable hydraulic jack accompanied by a reaction wall (see Figure 1(a)).
(2) The transverse steel pipe gallery is also pressed into place (see Figure 1(b)).
(3) A transversal slab is installed and filled with concrete and reinforced with rebar (see Figure 1(c)).
(4) Soil is excavated downward to create a trench, which is then lined with precast concrete walls (see Figure 1(d)).
(5) Concrete is poured to form a continuous vertical wall (see Figure 1(e)).
(6) The bottom slab is cast in concrete, and the railway track is placed (see Figure 1(f)).

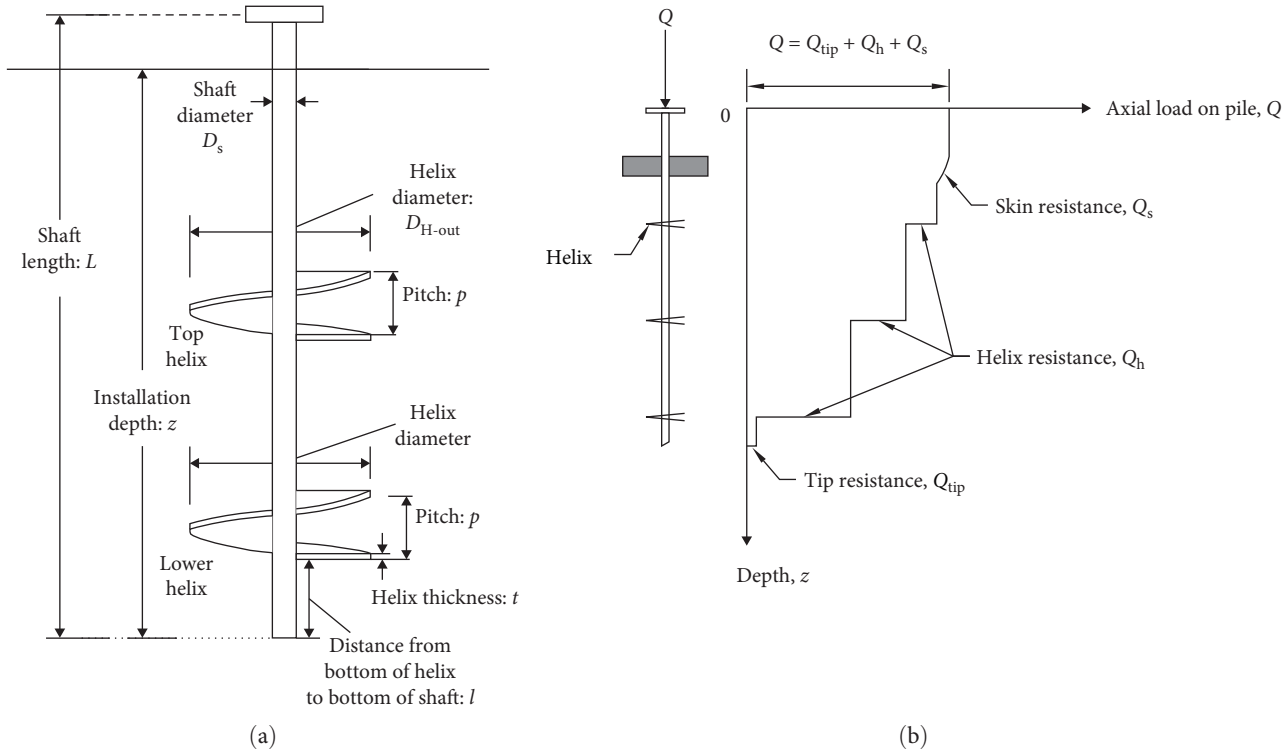

FIGURE 2: (a) Definition of helical pile and (b) load transfer model for helical piles.

3. Overview of Helical Piles and Interpretation of Load-Bearing Capacity Using HPCap Program

Helical piles, also known as screw piles, are deep foundations widely used to increase soil-bearing capacity in challenging soil conditions. The increasing use of helical piles due to the quick installation as well as its adaptability in various construction space constraints. These piles consist of a shaft with helix plates, and they are installed by rotating them into the ground, utilizing the resistance provided by the skin (Q_s), helix (Q_h), and tip (Q_{tip}) to transfer loads effectively (as depicted in Figure 2).

There are numerous factors that affect the performance of helical piles. This includes installation effects, which could usually affect the density of the soil above and between the helices. This was presented by Lutteneger and Tsuha [6], in which they reported that the tensile capacity of single helical piles can vary between 45% and 94% of the compressive capacity. Hence, in order to have a reasonable estimate of the helical pile tensile capacity, it is necessary to use suitable capacity factors that consider installation effects. In an effort to find a simpler way to determine the capacity of a helical pile considering installation effects, Hoyt et al. [7] and Tsuha and Aoki [8] implied that the torsional resistance which occurs as a result of the screw pile penetration, determined during installation, controls the capacity of the pile. Another factor that influences the behavior of a helical pile is the embedment depth of the helix. A deeper embedment of the helix leads to a greater enhancement of the helical pile's capacity. In addition, the embedment depth of the helix affects the values of the bearing capacity factors for estimating its ultimate axial capacity. Meyerhof [9] presented values of the bearing capacity factors of shallow and pile foundations and showed that the capacity factors of pile foundations are larger than strip and square footings.

Another important aspect of helical pile design is the determination of its behavior associated with its configuration. The spacing ratio (S_h/D_h), which is the ratio between the spacing between helices (S_h) and the average helix diameter (D_{have}), controls the failure mechanism and determines whether the cylindrical shear method or the individual bearing method is used. Nasr [10] suggested that a spacing ratio of greater than 2.0 is enough for the individual bearing method to be employed. However, recent studies have suggested that the boundary between the cylindrical shear method and the individual bearing method is at a spacing ratio of about 3.0. Aydin et al. [11] claim that this spacing ratio shifts the failure mechanism, and Luttenegger [12] demonstrated this by conducting numerous load tests, in which they showed that the piles with a spacing ratio of 3.0 have a large helix efficiency of about 90% in comparison to a spacing ratio of 2.25, which only showed an efficiency of about 65% at displacements of 20% the helix diameter. In a more recent study, Nowkandeh and Choobbasti [13] were able to recommend through finite element (FE) modeling that the spacing ratio in clay and sand should be 2.0 and 3.0, respectively. The following two modes of failures, as shown in Figure 3, are widely considered in calculations of helical piles bearing capacity:

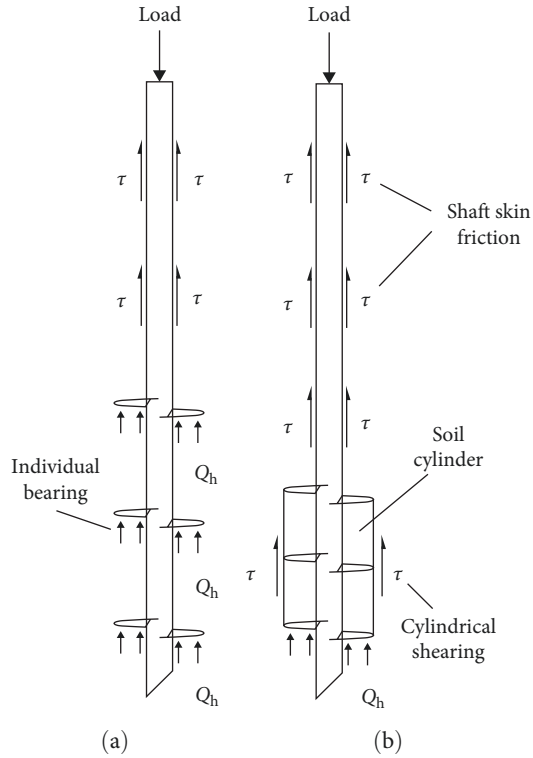

Figure 3: Mechanism of helical pile operation (a) cylindrical shear failure and (b) individual bearing failure.

(a) Individual bearing mode: This mode is shown in Figure 3(a); it can be seen that the spacing between helices is large, making each helix to behave independently. Therefore, the bearing capacity is calculated by summation of all helices bearing capacities.

(b) Cylindrical shear mode: This mode is shown in Figure 3(b); it can be seen that the spacing between helices is small, making helices behavior as a group. The bearing capacity of the helical pile results from the combined contributions of the bottom helical bearing plate and the side shear along the length of the cylinder created by the helical bearing plates [14].

Helical pile design codes are relatively scarce, with notable standards like the British Standard BS 8004:2015 [15] and the Canadian Foundation Engineering Manual CFEM 2006 [16] being among the few that have addressed this aspect. These codes outline methods for calculating the ultimate axial capacity of helical piles, providing crucial guidelines for engineers and designers in this specialized area. A summary of various methods of computations for helical piles, screw piles, and anchors can also be found in the publications by Das and Shukla [17], Chance and Atlas [18], Mohajerani et al. [19]. Nonetheless, the theoretical methods mentioned above allow for the calculation of the ultimate capacity of helical piles through equations that vary according to the loading type. The calculated values for these design methods should be compared with values from measured load tests, which involve not only the physical measuring of settlements and relative loads through the use of special equipment but also through theoretical interpretations of the graphs [19]. In addition, the soil profile at a particular site should be calibrated by field tests so that the methods of computation can be used with more confidence.

The HPCap (Helical Pile Capacity) program [20] has been developed by the geotechnical engineering lab at Kunsan National University in Gunsan, South Korea, to predict the axial and lateral behavior of helical piles based on the load transfer method. The current design methods for helical piles are limited at the estimation of the ultimate axial capacity, and the load–displacement of the behavior of a helical pile is commonly predicted by the use of the finite element method (FEM). Usually, helical piles are modeled in 3D space using FEM, and this can be time-consuming. Furthermore, commercial FE programs can be expensive. The program utilizes springs to replace the resistance provided by the soil, as shown in Figure 4. To determine the axial displacement at any point along the helical pile and to solve the problem of the distribution of load along the helical pile for a given applied load, the nonlinear differential equation shown in Equation (1) is solved by considering an element from the shaft, which is represented by length h.

$$\frac{\Delta w}{h} = \frac{Q}{EA}, \tag{1}$$

where w = movement of the pile; h = length of considered element; Q = load on the pile at the location of movement w; E = modulus of elasticity of the pile material; A = cross-sectional area of the pile.

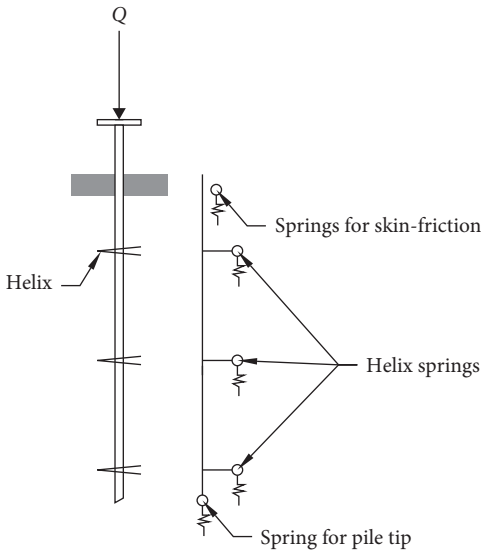

Figure 4: HPCap beam spring approach for static compression loading.

In the literature, there exist numerous capacity factors for axially loaded non-helical piles and helical piles. In addition, the displacement criteria also vary from research to research. The bearing capacity factors and the displacement criteria are the two very important aspects of the load transfer method. The authors do not directly suggest the use of capacity factors and load transfer curves from one particular research mainly because capacity factors and load–displacement behavior vary from site to site and the helical pile configuration. In the HPCap program, user inputs for various capacity factors are allowed to make sure that the calculation of the ultimate capacity can be flexible based on field observations. Numerous factors that have already been introduced in the literature have been baked into HPCap to provide further flexibility. Limiting end-bearing values and shaft friction values have also been incorporated in HPCap. In the axial analysis using HPCap, the helical pile is divided into 150 nodes or 149 segments, and the stiffness of the springs is represented by the load transfer curves. As discussed above, there exist numerous load transfer curves for the shaft resistance and tip resistance, including those from the American Petroleum Institute [21]; however, the spring stiffness for helical resistance has not been proposed in the literature. In HPCap, the spring stiffness for helical resistance was derived from full-scale axial compression and uplift tests conducted by Sakr [22] on large-capacity helical piles in cohesionless soils.

4. Case Study

During the construction of the Seolleung Station on the Bundang Green Line in Seoul, South Korea (Figure 5), several challenges were faced, including heavy traffic, existing tall buildings nearby, and soft ground conditions. To overcome these issues, the TRcM method was employed for tunnel construction, which provided advantages such as smooth

Figure 5: Project location map.

traffic flow on the surface and stability for nearby structures against settlement.

The subsurface geological investigations (see Figure 6) revealed that the soft ground had low bearing capacity for the TRcM construction, necessitating ground improvement measures. Moreover, the limited space and time constraints further complicated the situation due to the soft ground conditions. To address these challenges and enhance the axial compression bearing capacity beneath the TRcM, the implementation of helical piles for ground improvement was proposed. The plan and section elevations of the site are shown in Figure 7.

First, inside the TRcM, a standard penetration test (SPT) [23] was conducted, and the corrections were applied to calculate N_{60} and $(N_1)_{60}$ [24, 25] and the soil profile at the site based on the SPT is shown in Figure 6(a). The values of N, N60, and (N1)60 at depths 0–5.0 m range from 7.0 to 8.0, 5.0 to 6.0, and 6 to 10, respectively. At depths 6.0–10.0 m, the values of N, N60, and (N1)60 range from 7.0 to 15.0, 5.0 to 18.0, and 5.0 to 15.0, respectively, while for depths greater than 10.0 m, the values range from 23.0 to 50.0, 16.0 to 36.0, and 15.0 to 28.0, respectively. Additionally, the collected SPT samples from different depths in the borehole were used to perform soil gradation tests [26] to classify as per unified soil classification system [27]. As shown in Figure 6(b), the site consists of sand, silty sand, and clayey sand. The water table at the site was located at a depth of 4.5 m. The compaction tests [28] were performed on the SPT samples to calculate the unit weight of soil [29], as shown in Figure 6(c). Also, the

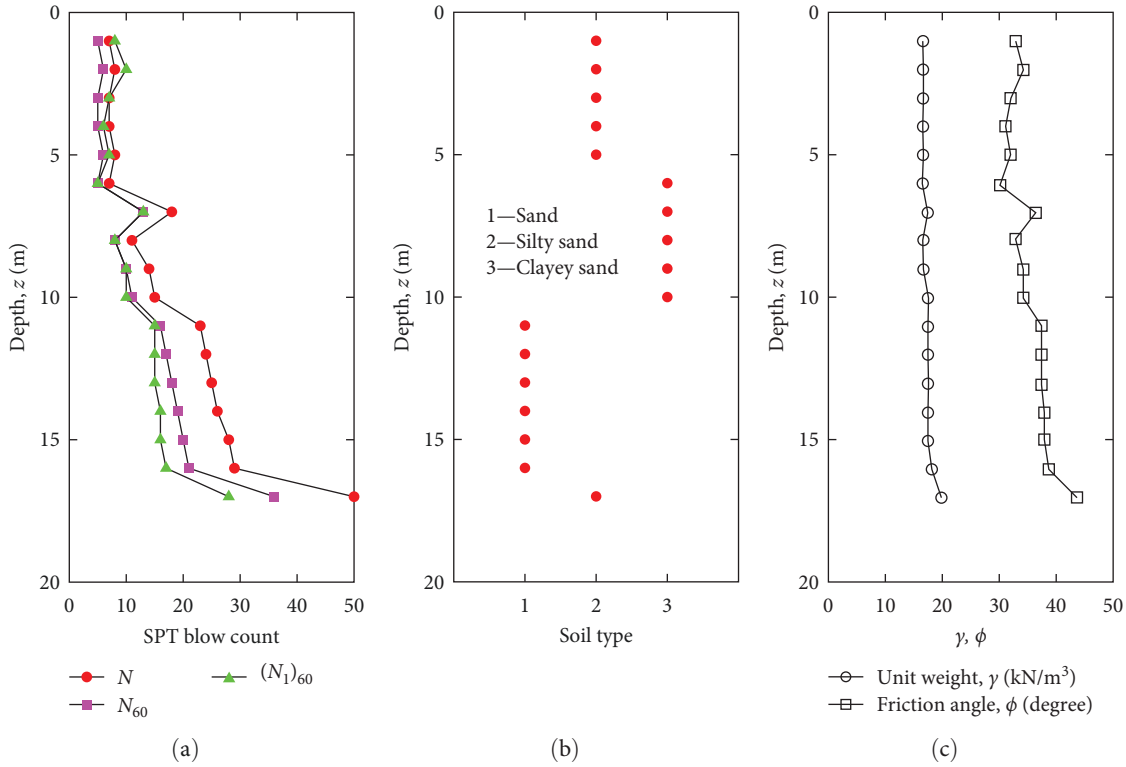

Figure 6: Soil profile of underground site based on standard penetration test (SPT): (a) SPT blow count with depth, (b) soil type with depth, and (c) soil unit weight and friction angle with depth.

Hatanaka and Uchida [30] empirical correlation was used to calculate the friction angle of the soil profile, as shown in Figure 6(c).

A customized machine TRPM-08 was developed and manufactured, which was capable of installing helical piles from 1.6 m diameter gallery pipe (Figure 8(a)); the properties of steel pipe are presented in Table 1. First, a helical test pile for the static pile load test was installed. The static helical pile test assembly setup is shown in Figure 9. The axial capacity calculation methods were evaluated by comparison with the measured field pile load test. The helical piles used inside the TRcM plan and the section elevations are shown in Figure 7(b). These piles were of four helices, each spaced at 1.8 m, having embedment depth and diameter of 8 m and 165.2 mm, respectively. These were installed at a spacing of 1.5 m center to center below the TRcM vertical trench wall, which was later filled with concrete. A summary of the properties of the helical pile at the TRcM site is given in Table 2.

To conduct compression static test according to ASTM D1143 [31], a testing frame assembly was designed as shown in Figures 9(a) and 9(b). This assembly comprises a reaction plate, a loading device, and a measuring system. The reaction system consists of a 30 mm thick steel reinforcing plate for smooth and safe transfer of reaction to steel pipe. The system for loading comprises a load cell connected to a hydraulic jack through adaptors using internal cables. The hydraulic jack can be moved upward and downward using a remote control that connects to the hydraulic motor. The hydraulic motor supplies fluid to the hydraulic jack, applying the necessary pressure. The entire unit is aligned vertically along the central axis of the testing pile. The measuring equipment setup includes reference beams and dial gauges to measure the vertical displacement. Two dial gauges provide an average measurement of the vertical displacement, as shown in Figure 9.

One of the challenges in conducting pile static load tests inside constraint space was the safe engineering design of the testing assembly. Therefore, a customized analysis to assess the stability of the TRcM steel pipe was performed by simulation in MIDAS/GTS NX FE software [32]. The reaction arm with the TRcM pipe simulation model and used physical properties of the steel are presented in Figure 9(c) and Table 1, respectively. The plate element was used to simulate the TRcM pipe, reaction reinforcing plate as well as reaction arm all were simulated using the plate element. The reaction beam was loaded to 140 tonf of static pile loading and the surface train load of 5 ton/m^2. The TRcM pipe diameter and thickness were 2,500 and 25 mm, respectively, whereas the steel reinforcing plate in the reaction beam was 30 mm thick. The stability analysis of the reaction arm system is discussed in Section 5.

The static test helical pile result was simulated using the HPCap software to evaluate various helical pile capacity estimation factors such as mode of failures, lateral earth pressure coefficient (K_c), bearing capacity factor (N_q), and interface angle (δ). The soil profile and the helical pile properties simulated in HPCap are shown in Figure 6 and Table 2, respectively. The HPCap results are discussed in Section 5.

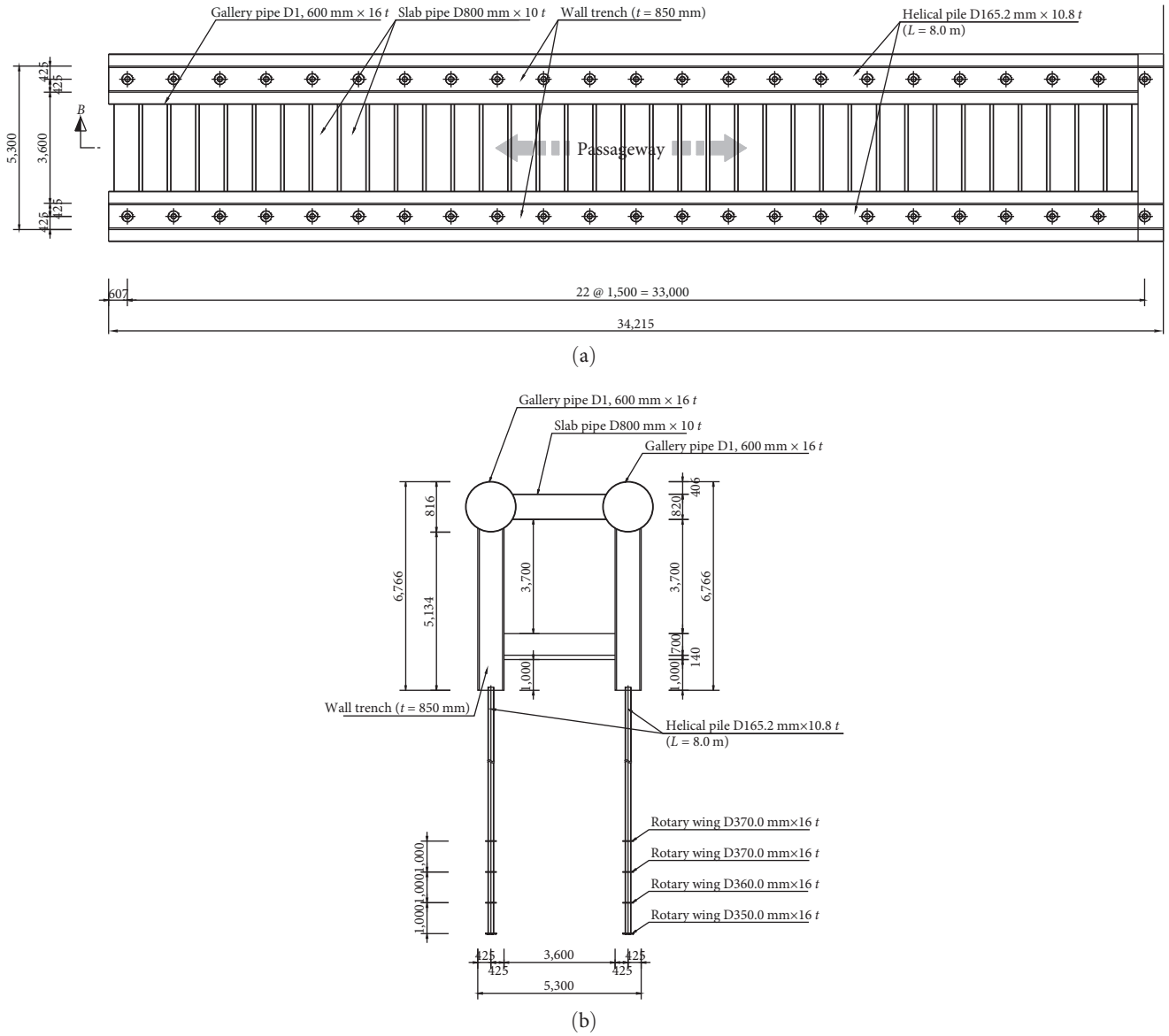

Figure 7: Case study site showing TRcM and helical pile (a) plan and (b) sectional elevation.

(a) (b) (c)

Figure 8: (a) Customized machine TRPM-08 for helical pile installation, (b) working of TRPM-08 machine inside TRcM pile, and (c) static pile load test loading devise with reaction frame and LVDTs.

5. Results and Discussion

Figure 10 shows the results of the numerical stability analysis results of the reaction arm on TRcM pipe in terms of normal stresses (compression and tension) and tensile stress. During the pile load test, the compressive stress of the steel pipe was 64.86 MPa (allowable stress 210 MPa [33]), the maximum

Table 1: Physical properties of steel.

Steel	Modulus of elasticity (MPa)	Unit weight (kN/m^3)	Poisson's ratio (ν)	Allowable compressive stress (MPa)	Allowable tensile stress (MPa)	Allowable shear stress (MPa)
STK400	210,000	78.5	0.3	210	210	120

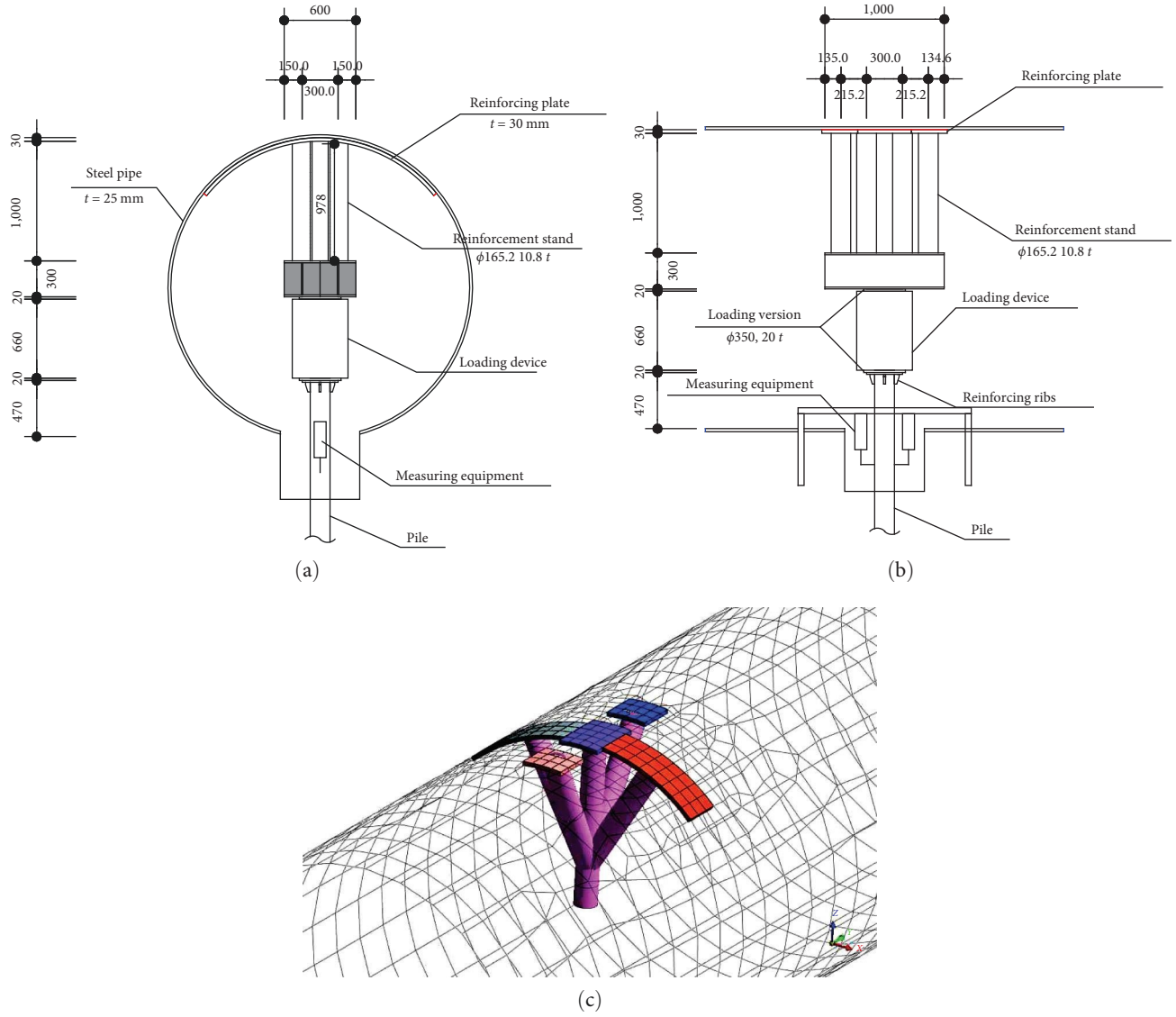

Figure 9: Static helical pile load test assembly (a) cross-sectional details, (b) longitudinal section details, and (c) simulated stability analysis domain in MIDAS program.

Table 2: Properties of the helical pile at the underground site.

Sr no.	Pile properties	Quantity
01	Pile length, L (m)	9.23
02	Pile shaft diameter, D_p (mm)	165.2
03	Pile thickness, t (mm)	10.8
04	Modulus of elasticity, E (kPa)	210,000,000
05	Length of embedment, L_{embed} (m)	8.68
06	First helix diameter, D_{h1} (mm)	370
07	Second helix diameter, D_{h2} (mm)	370
08	Third helix diameter, D_{h3} (mm)	350
09	Fourth helix diameter, D_{h4} (mm)	350
10	Depth of first helix, z_{h1} (m)	5.5
11	Helix spacing, S_h (m)	1.0

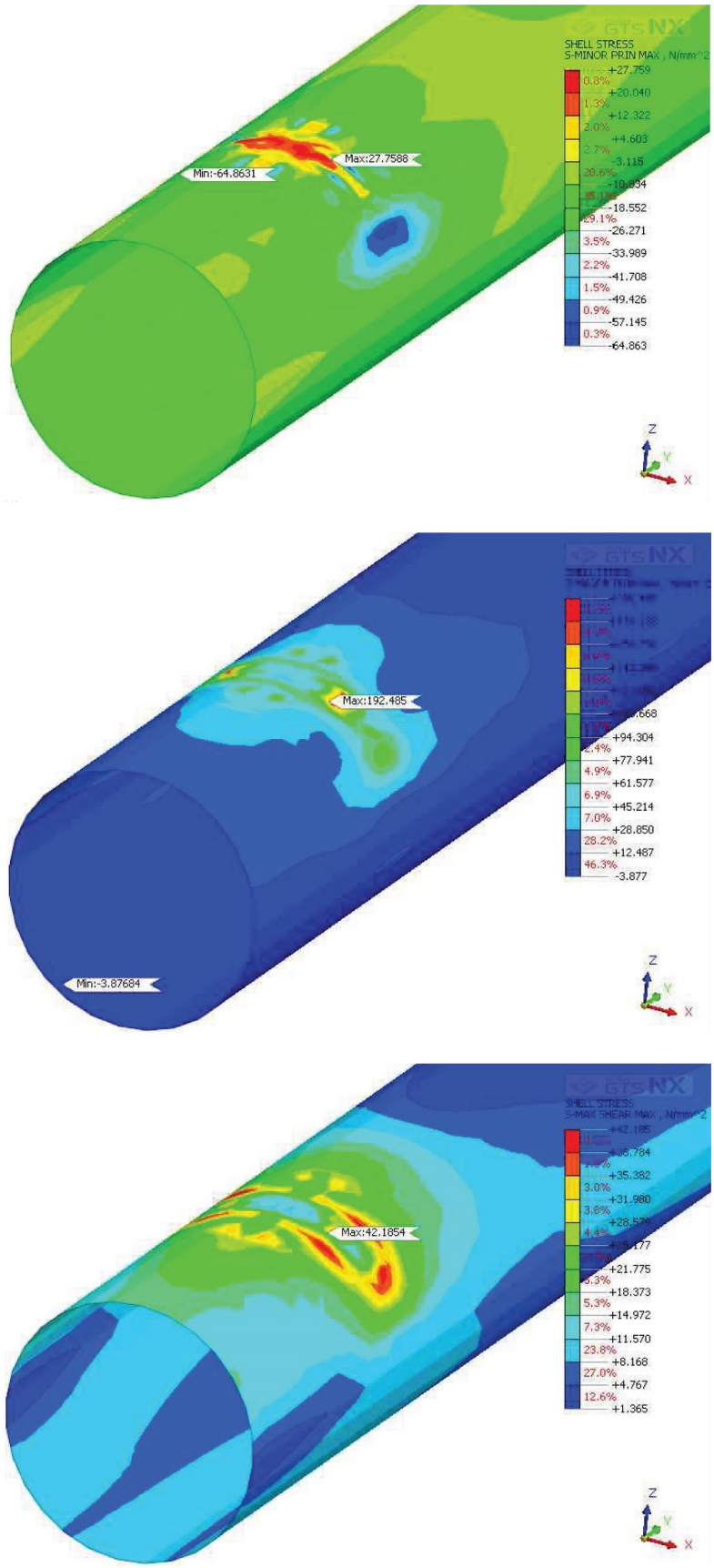

Figure 10: Numerical stability analysis results of reaction arm on TRcM pipe.

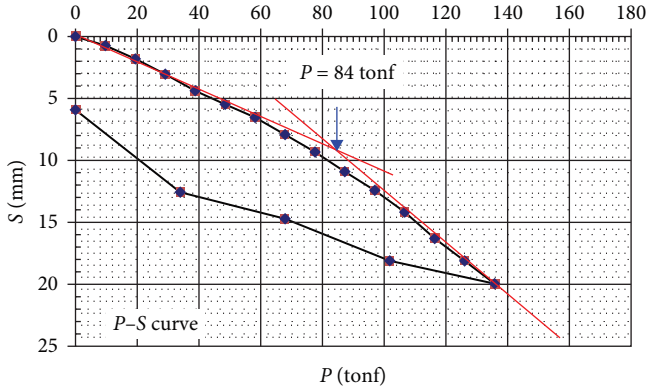

Figure 11: Measured load–displacement curve of static helical pile load test.

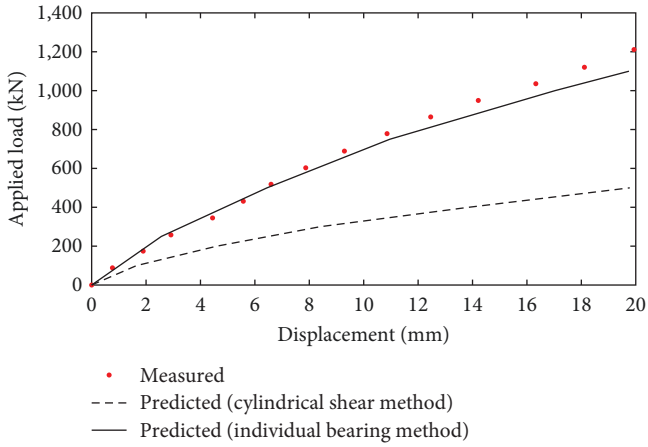

Figure 12: Effect of mode of failure on the estimation of bearing capacity.

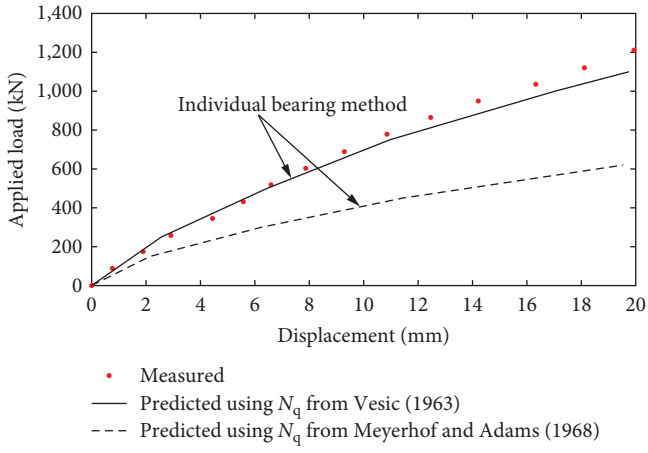

Figure 13: Effect of bearing capacity factor (N_q) on the estimation of bearing capacity (individual bearing capacity mode of failure).

tensile stress was 192.49 MPa (allowable stress 210 MPa [33]), and the maximum shear stress was 42.19 MPa (allowed 120 MPa [33]). It is evident that that the level of all stresses are in well agreement with the allowable limits, confirming the stability of the designed helical pile load assembly inside the TRcM.

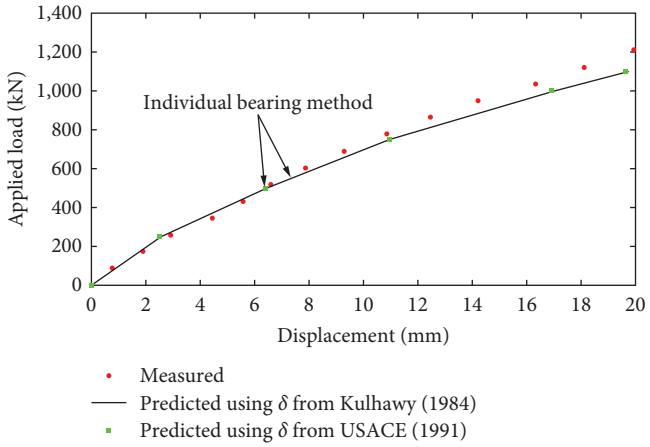

Figure 14: Effect of interface angle (δ) on the estimation of bearing capacity (individual bearing capacity mode of failure).

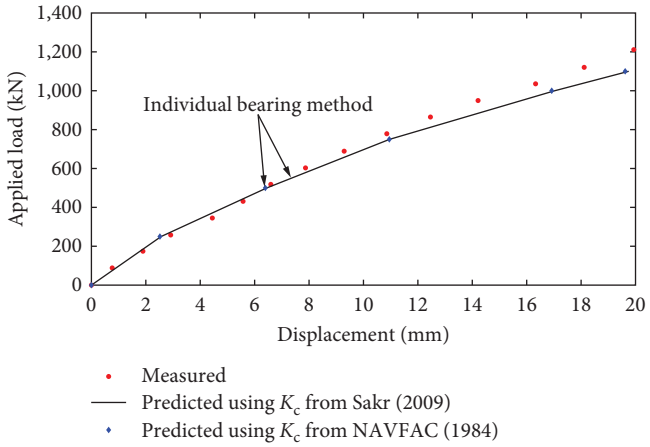

Figure 15: Effect of lateral earth pressure coefficient (K_c) on the estimation of bearing capacity (individual bearing capacity mode of failure).

After confirming the stability of reaction assembly, the static pile load test (Figure 8(c)) was performed on installed helical pile test according to ASTM and the load displacement curve is shown in Figure 11. The maximum test load was 140 tons and the corresponding settlement of 19.96 mm, whereas the residual settlement was 5.93 mm. As shown in Figure 11, the static load–displacement curve does not exhibit a clear ultimate point, therefore the axial capacity is calculated by extending the linear elastic portion of the curve and the yield portion of the curve until both intersects, that was found to be 84 tons with 9 mm of settlement. This static helical pile load test was utilized in calibration of the HPCap software.

The results of the helical pile static load test simulations are shown in Figures 12, 13, 14, and 15. In Figure 12, it can be seen that using the cylindrical shear method resulted in the underestimation of the capacity of the helical pile, and that the individual bearing method was more suitable even though the helix spacing ratio (S_h/D_h) was less than 3.0 for all helices. Nowkandeh and Choobbasti [13], recommend through FE

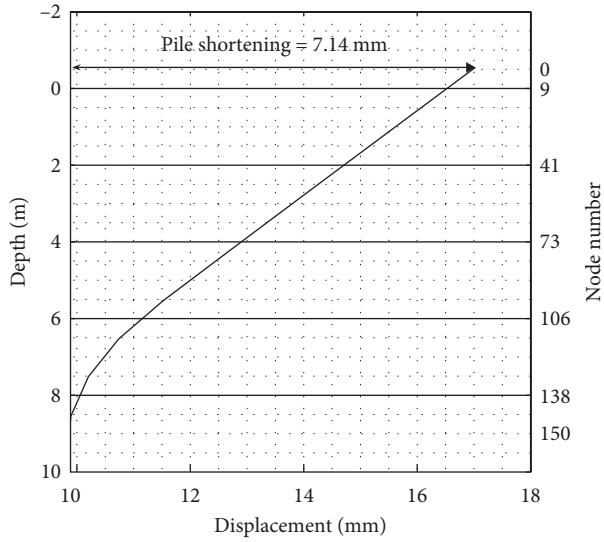

Figure 16: Displacement distribution along the depth or nodes of the helical pile at an axial load of 1,000 kN.

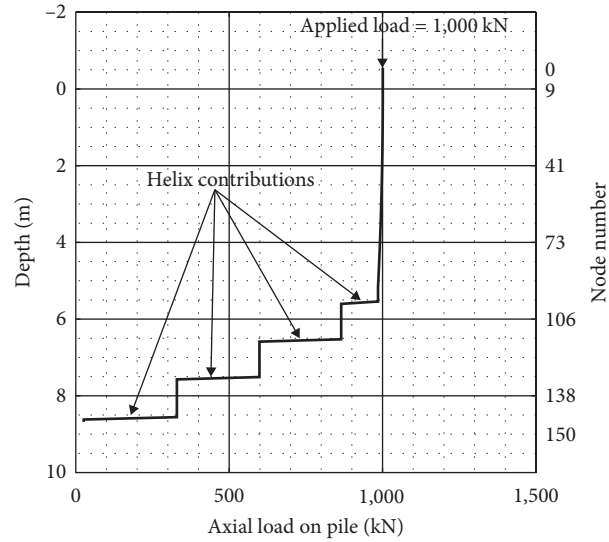

Figure 17: Axial load distribution along the depth or nodes of the helical pile at an axial load of 1,000 kN.

modeling that the distance between helices in clay and sand should be $2D_h$ and $3D_h$, respectively, to attain high helix efficiency. However, in the pile load test, high helix efficiency was observed at an average spacing of about $2.78D_h$, which is still close to a spacing of $3D_h$. Therefore, reliance on a spacing limit may sometimes be inadequate in assessing the capacity of helical piles. In addition, the mode of failure used in the simulation must represent the behavior in the field.

To evaluate the effect of the bearing capacity factor N_q, capacity factors proposed by Vesic [34] and Meyerhof and Adams [35] are compared in Figure 13. It can be seen that the predicted load–displacement curve by Meyerhof and Adams [35] was underestimated by factor of 1.66. It should be noted that N_q from Vesic [34] provides large values, and it is usually recommended for pile tips located at 10 times the pile diameter (D_p). Interestingly, the first helix was located at 14.86 times the helix diameter (14.86 x 0.37 m = 5.5 m), hence, N_q proposed by Vesic [34] was suitable.

The effect of both interface angle (δ) [36] and coefficient lateral pressure (K_c) [22, 37] on bearing capacity calculations are shown in Figures 14 and 15, respectively. It can be seen that both has minimal effect on the estimates. This is because shaft friction resistance provided by the pile was minimal due to the pile shaft diameter only being 165.2 mm. The shaft friction resistance was estimated to be at the range of 20–30 kN.

Using the calibrated parameters, Figures 16 and 17 depict the distributions of displacement and axial load along the depth or nodes of the helical pile under an axial load of 1,000 kN, respectively. As depicted in Figure 16, the HPCap program predicts a total displacement of approximately 17 mm at the pile head. Analyzing the displacement distribution reveals a total pile shortening of about 7 mm, underscoring the significance of considering pile shortening in helical pile design, particularly under heavy loads. Examining Figure 17, it is evident that the resistance against the 1,000 kN applied load is primarily provided by the helices, with the tip and skin-friction resistance playing a minor role. Moreover, Figure 17 illustrates that the top-most helix contributes only about 50% of the capacity of the helices below it.

6. Conclusion

This paper presents a case study of using of Seolleung Station construction on the Bundang Line in Seoul, South Korea, several challenges were faced, including heavy traffic, existing tall buildings nearby, and soft ground conditions. To overcome these issues, the TRcM with helical piles was employed for tunnel construction. The study presents the unique static helical pile test setup inside the TRcM. The stability analysis and the simulation of static compression helical pile capacity were performed using the MIDAS and HPCap program, respectively. As a result of the analysis, the following conclusions were obtained:

(1) The stability analysis of designed loading arm on TRcM pipe confirm that compressive stress (64.86 MPa), tensile stress (192.49 MPa), and shear stress (42.19 MPa) during the pile load test are within allowable limits (210 MPa for compressive and tensile, 120 MPa for shear), affirming the stability of the proposed helical pile load assembly inside the TRcM.

(2) The static helical pile load test conducted inside the TRcM resulted in a maximum load of 140 tons, settlements of 19.96 mm under load and 5.93 mm residual, and an axial capacity of 84 tons with 9 mm settlement, providing essential calibration data for the HPCap software.

(3) The simulation of helical pile load test using HPCap reveals that the selection of the appropriate mode of failure and bearing capacity factors have governing effect, whereas the lateral earth pressure coefficient and the interface angle are shown to be insensitive. The individual bearing method and Vesic [34]

bearing capacity factors captured the measured load displacement curve.

The analysis of displacement and axial load distributions along the helical pile under a 1,000 kN load underscores the importance of accounting for pile shortening, with a predicted 17 mm displacement at the pile head and approximately 7 mm pile shortening. Furthermore, the examination reveals that the helices predominantly contribute to load resistance, with the top-most helix contributing only about 50% of the individual capacity of the other three helices. Given space and time constraints during installation, it is advisable to consider the use of helical piles as a ground improvement method alongside TRcM. Additionally, the presented design of static helical assembly load test is safe and can be utilized in engineering practice.

Data Availability

Data will be made available upon request.

Conflicts of Interest

The authors declare that they have no conflicts of interest.

Acknowledgments

This research was supported by the Basic Science Research Program through the National Research Foundation of Korea (NRF), funded by the Ministry of Education (NRF2021R1A6A1A1A03045185, Brain Korea 21 FOUR) and by the Human Resources Development of the Korea Institute of Energy Technology Evaluation and Planning (KETEP) grant funded by the Korean Government (Ministry of Trade, Industry & Energy) (no. 20214000000180).

References

[1] G. Musso, "Jacked pipe provides roof for underground construction in busy urban area," *Civil Engineering*, vol. 49, no. 11, pp. 79–82, 1979.

[2] P. Lunardi, "The cellular arch method: technical solution for the construction of the Milan railway's venezia station," *Tunnelling and Underground Space Technology*, vol. 5, no. 4, pp. 351–356, 1990.

[3] Y.-B. Lee, J.-Y. Kim, I.-J. Park, K.-G. Kim, and J.-H. Lee, "A study on the applicability of under ground structure using steel tubular roof in Korean geotechnical condition," *Journal of Korean Tunnelling and Underground Space Association*, vol. 5, no. 4, pp. 401–409, 2003.

[4] X. Li, Z. Tan, X. Wang, and K. Lei, "Comparative study on the influence of different forms of new tubular roof method construction on railway tracks," *Symmetry*, vol. 14, no. 7, Article ID 1361, 2022.

[5] X. Yang and Y. Li, "Research of surface settlement for a single arch long-span subway station using the pipe-roof pre-construction Method," *Tunnelling and Underground Space Technology*, vol. 72, pp. 210–217, 2018.

[6] A. J. Lutenegger and C. de Tsuha, "Evaluating installation disturbance from helical piles and anchors using compression and tension tests," in *Proceedings of the XV Pan-American Conference on Soil Mechanics and Geotechnical Engineering*, pp. 373–381, IOS Press, 2015.

[7] R. M. Hoyt, A. Chance, and S. P. Clemence, "Uplift capacity of helical anchors in soil," in *Congrès International de Mécanique des Sols et des Travaux de Fondations*, vol. 12, pp. 1019–1022, A. A. Balkema Publishers, 1989.

[8] C. de Hollanda Cavalcanti Tsuha and N. Aoki, "Relationship between installation torque and uplift capacity of deep helical piles in sand," *Canadian Geotechnical Journal*, vol. 47, no. 6, pp. 635–647, 2010.

[9] G. G. Meyerhof, "Some recent research on the bearing capacity of foundations," *Canadian Geotechnical Journal*, vol. 1, no. 1, pp. 16–26, 1963.

[10] M. Nasr, "Performance-based design for helical piles," in *Contemporary Topics in Deep Foundations*, pp. 496–503, ACM, 2009.

[11] M. Aydin, T. D. Bradka, and D. A. Kort, "Osterberg cell load testing on helical piles," in *Geo-Frontiers 2011: Advances in Geotechnical Engineering*, pp. 66–74, ACM, 2011.

[12] A. J. Lutenegger, "Behavior of multi-helix screw anchors in sand," in *Proceedings of the 14th Pan-American Conference on Soil Mechanics and Geotechnical Engineering*, p. 126, 2011.

[13] M. J. Nowkandeh and A. J. Choobbasti, "Numerical study of single helical piles and helical pile groups under compressive loading in cohesive and cohesionless soils," *Bulletin of Engineering Geology and the Environment*, vol. 80, pp. 4001–4023, 2021.

[14] H. A. Perko, *Helical Piles: A Practical Guide to Design and Installation*, John Wiley & Sons, 2009.

[15] British Standard, *8004 Code of Practice for Foundations*, British Standards Institution, London, 2015.

[16] C. G. Society, *Canadian Foundation Engineering Manual*, BiTech Publishers Ltd., Richmond, B. C, 4th edn edition, 2006.

[17] B. M. Das and S. K. Shukla, *Earth Anchors*, J. Ross Publishing, 2013.

[18] Chance and Atlas, *Technical Design Manual*, Hubbell Power Systems, Inc., 3rd edition, 2014.

[19] A. Mohajerani, D. Bosnjak, and D. Bromwich, "Analysis and design methods of screw piles: a review," *Soils and Foundations*, vol. 56, no. 1, pp. 115–128, 2016.

[20] H.-J. Kim, P. R. Dinoy, J. V. Reyes, H. Kim, J.-Y. Kim, and T.-W. Park, "Analysis of axially loaded helical piles in sand using HPCap program," in *The 2021 World Congress on Advances in Structural Engineering and Mechanics (ASEM21)*, pp. 1–7, Techno-Press, GECE, Seoul, Korea, August 2021.

[21] API 2A-WSD, "Recommended practice for planning, designing and constructing fixed offshore platforms-working stress design," USA, Dezembro, 2000.

[22] M. Sakr, "Performance of helical piles in oil sand," *Canadian Geotechnical Journal*, vol. 46, no. 9, pp. 1046–1061, 2009.

[23] D1586/D1586M-18e1 A, "Standard test method for standard penetration test (SPT) and split-barrel sampling of soils".

[24] A. W. Skempton, "Standard penetration test procedures and the effects in sands of overburden pressure, relative density, particle size, ageing and overconsolidation," *Géotechnique*, vol. 36, no. 3, pp. 425–447, 1986.

[25] H. B. Seed, K. Tokimatsu, L. F. Harder, and R. M. Chung, "Influence of SPT procedures in soil liquefaction resistance evaluations," *Journal of Geotechnical Engineering*, vol. 111, no. 12, pp. 1425–1445, 1985.

[26] D6913-04(2009)e1 A, "Standard test methods for particle-size distribution (Gradation) of soils using sieve analysis".

[27] D2487-17 A, "Standard practice for classification of soils for engineering purposes (unified soil classification system)".

[28] D1557-12 A, "Standard test methods for laboratory compaction characteristics of soil using modified effort," 2021.
[29] D7263-21 A, "Standard test methods for laboratory determination of density and unit weight of soil specimens".
[30] M. Hatanaka and A. Uchida, "Empirical correlation between penetration resistance and internal friction angle of sandy soils," *Soils and Foundations*, vol. 36, no. 4, pp. 1–9, 1996.
[31] ASTM-D1143, "Standard test methods for deep foundation elements under static axial compressive load," 2020.
[32] MIDAS and InformationTechnology, "Midas GTS NX 2014 v2.1 analysis reference," 2014.
[33] Korean Standards Association, "KS D 3566: carbon steel tubes for general structural purposes," 2010.
[34] A. B. Vesic, "Bearing capacity of deep foundations in sand," Highway research record (39), 1963.
[35] G. G. Meyerhof and J. I. Adams, "The ultimate uplift capacity of foundations," *Canadian Geotechnical Journal*, vol. 5, no. 4, pp. 225–244, 1968.
[36] F. Kulhawy, "Critical evaluation of design methods for foundations under axial uplift and compression loading," Final report. Cornell Univ., Ithaca, NY (USA). Geotechnial Engineering Group, 1984.
[37] NAVFAC Design Manual 7.2, "Foundation and earth structures," US Department of the Navy, 1984.